Effects of Annealing and Pressure on Devitrification and Mechanical Properties of Amorphous $Al_{87}Ni_7Gd_6$

P. WESSELING, B.C. KO, L.O. VATAMANU, G.J. SHIFLET, and J.J. LEWANDOWSKI

Annealing studies at different temperatures, as well as those conducted with 940 MPa hydrostatic pressure, were conducted on amorphous ribbons of $Al_{87}Ni_7Gd_6$. The studies were performed to investigate the evolution of structure under different conditions and to particularly examine the effects of superimposed hydrostatic pressure during annealing. This amorphous alloy devitrifies at low temperatures *via* the precipitation of nano-crystalline α-Al particles. The effects of these various exposures on the amount of devitrification have been quantified using a variety of analytical techniques (*i.e.*, X-ray diffraction (XRD), differential scanning calorimetry (DSC), and transmission electron microscopy (TEM)). In addition, the effects of devitrification on the mechanical properties have been quantified using microhardness indentation and uniaxial tension tests.

DOI: 10.1007/s11661-007-9384-2

I. INTRODUCTION

SIGNIFICANT interest in amorphous and nanocrystalline aluminum alloys has existed because of the early discoveries of amorphous aluminum alloys[1] and reviews of the balance of properties[2] possible in such systems. Recent work has focused on the Al-Ni-Gd system and variants[3,4] to explore processing paths for the creation of useful materials with a balance of properties. In this regard, the effects of annealing conditions (*i.e.*, temperature, pressure, and time) were explored to determine the range of properties possible with controlled treatments and to compare these to recent reviews of properties.[2]

A few studies have investigated the evolution of structure,[5,6] with annealing, while much less work has been conducted to examine the effects of superimposed pressure on structure evolution and resulting properties. This may have importance in the processing of these materials as well as provide insight to the mechanisms of devitrification, because both acceleration[7–9] and deceleration[10–12] of kinetics have been reported in different systems. The present work was undertaken in order to extend our previous work[3,13,14] in these areas, while comparing results to other investigations.[2,6–12]

P. WESSELING, formerly Student, Department of Materials Science and Engineering, Case Western Reserve University, is Metallurgical Engineer with McWilliams Forge Inc., Rockaway, NJ 07866, USA. B.C. KO, Research Associate, and J.J. LEWANDOWSKI, Leonard Case, Jr., Professor of Engineering, are with the Department of Materials Science and Engineering, Case Western Reserve University, Cleveland, OH 44106, USA. Contact e-mail: jjl3@case.edu L.O. VATAMANU, formerly Research Associate, Department of Materials Science and Engineering, Case Western Reserve University, Cleveland, USA, is Senior Research Scientist with Powdermet Inc., Euclid, OH 44117 USA. G.J. SHIFLET, William G. Reynolds Professor, is with the Department of Materials Science and Engineering, University of Virginia, Charlottesville, VA 22904, USA.

This article is based on a presentation given in the symposium entitled "Bulk Metallic Glasses IV," which occurred February 25–March 1, 2007 during the TMS Annual Meeting in Orlando, Florida under the auspices of the TMS/ASM Mechanical Behavior of Materials Committee.

Article published online December 21, 2007

II. MATERIALS AND EXPERIMENTAL PROCEDURES

The amorphous ribbons ($Al_{87}Ni_7Gd_6$) were produced *via* melt spinning using a chilled copper block at two different speeds, *i.e.*, 2900 and 1000 RPM.[15] The ribbons had a thickness of approximately 25 and 33 μm, respectively. Ribbon materials were stored under refrigeration to minimize diffusion-related changes at room temperature, while characterization by X-ray diffraction (XRD), differential scanning calorimetry (DSC), and transmission electron microscopy (TEM) was performed, as described by Ko *et al.*[3]

Isothermal annealing treatments were conducted on 30- to 40-mm-long individual specimens for 30 minutes in silicone oil (GE, USEP SF 1147) maintained at 123 °C, 145 °C, 158 °C, 173 °C, 188 °C, 191 °C, 205 °C, 232 °C, and 262 °C in an Innovare hydrostatic extrusion rig.[16] Additional isothermal annealing experiments were conducted at 123 °C, 145 °C, 158 °C, 173 °C, 188 °C, 191 °C, 205 °C, and 232 °C in oil, which was maintained at 940 MPa superimposed pressure in the Innovare hydrostatic extrusion rig. Experimental details are described by Wesseling *et al.*[13] The total time at temperature was constant for both the atmospheric pressure and high pressure tests. Subsequent analyses and mechanical testing were conducted on both as-received (*i.e.*, as melt spun) and annealed ribbons.

Mechanical properties were obtained by several testing techniques. A Buehler microhardness machine (Buehler Ltd., Lake Bluff, IL) with a load of 50 g was used to measure the microhardness of the ribbon specimens. Uniaxial tensile tests and single edge-notched tension tests were also performed on specially designed specimens. Details of the microhardness and tensile tests were

described by Wesseling *et al.*[13] Scanning electron microscopy (SEM) was performed using a PHILIPS*

*PHILIPS is a trademark of Philips Electronic Instruments Corp., Mahwah, NJ.

XL-30 environmental scanning electron microscope at 15 kV on fracture surfaces of the tensile test specimens.

III. RESULTS

The XRD results for the as-received and ribbon specimens isothermally annealed for 30 minutes at atmospheric pressure are provided in Figure 1. Figure 2 presents the results for the as-received and ribbon specimens isothermally annealed for 30 minutes with 940 MPa pressure. The as-received ribbons exhibited a characteristic broad peak centered at an angle (2θ) of 38 deg. Isothermal annealing for 30 minutes at temperatures from 123 °C to 158 °C shows a decrease in intensity of this broad peak. For isothermal annealing temperatures larger than 158 °C, the broad peak sharpened. This sharpened peak corresponds to the reflection of the X-ray beam with the (111) plane of fcc aluminum and is located at an angle (2θ) of 38.5 deg. The corresponding d spacing calculated using the Bragg law of diffraction is 2.34 Å. Isothermal annealing at temperatures of 205 °C and greater shows evolution of secondary peaks at angles (2θ) of 44.8, 65.2, and 78.2

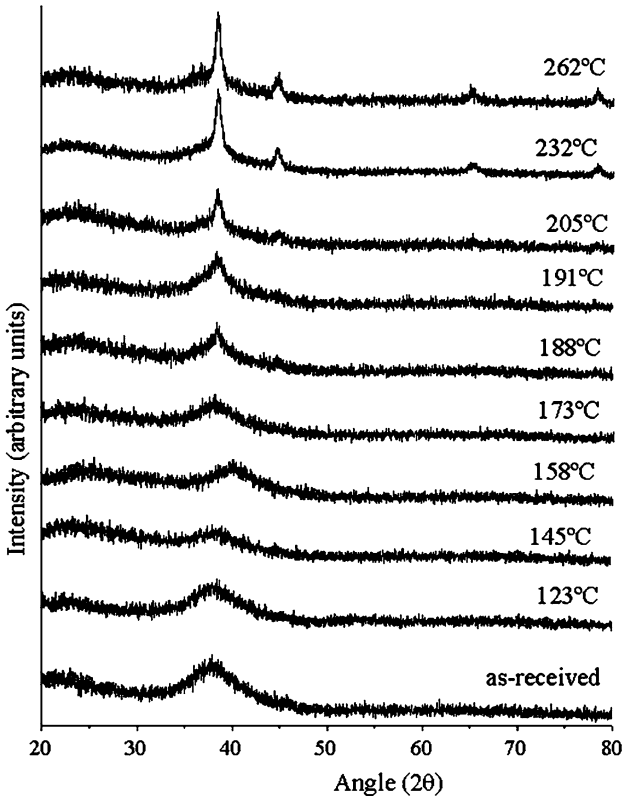

Fig. 1—XRD scans for ribbon specimens annealed for 30 min at atmospheric pressure.

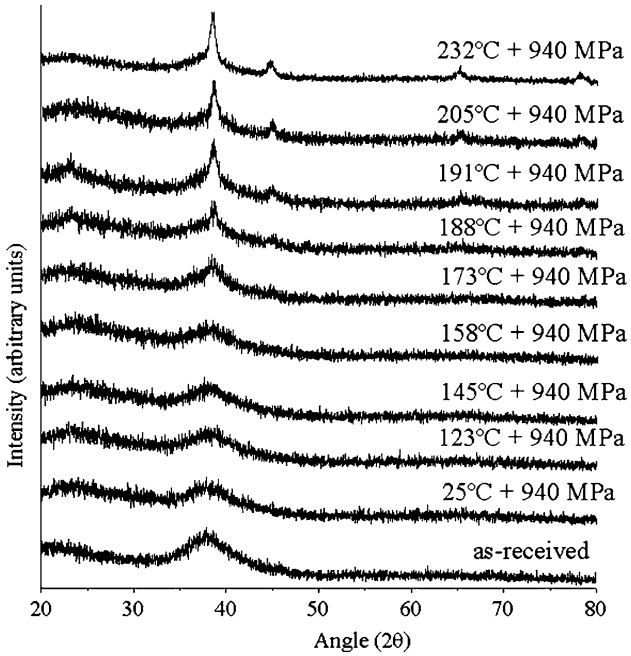

Fig. 2—XRD scans for ribbon specimens annealed for 30 min with 940 MPa pressure.

deg. These peaks correspond to the reflection of the X-ray beam with the (200), (220), and (311) planes of aluminum, respectively. The corresponding calculated d spacings of the planes are 2.02, 1.43, and 1.22 Å, respectively. The lattice parameters of the fcc unit cell for aluminum using the calculated d spacings and the diffraction planes (111), (200), (220), and (311) are 4.045, 4.042, 4.042, and 4.049 Å, respectively, calculated from the aforementioned planes.

Specimens annealed for 30 minutes with 940 MPa hydrostatic pressure at temperatures greater than 158 °C exhibited sharpening of the first broad peak. Annealing with pressure also enhanced the evolution of secondary peaks, as illustrated by comparing the X-ray scans of the specimens annealed at 191 °C and 205 °C with and without superimposed pressure (Figures 1 and 2).

The continuous DSC scans exhibited three exothermic peaks with peak temperatures of T_{p1} = 223 °C, T_{p2} = 330 °C, and T_{p3} = 363 °C. The first and second peaks correspond to the formation of fcc aluminum nanocrystals, while the third peak corresponds to the formation of intermetallics.[3,4,6] The as-received ribbon, *i.e.*, as-melt-spun specimen exhibited an onset temperature for the first peak of T_{x1} = 189 °C. The DSC traces for the as-received and ribbons isothermally annealed for 30 minutes at atmospheric pressure are provided in Figure 3. Figure 4 summarizes the DSC traces for the as-received ribbon and those isothermally annealed for 30 minutes with 940 MPa pressure. The onset and peak temperatures of the first peak significantly change, as summarized in Figure 5. For annealing temperatures less than or equal to 158 °C, the peak temperature and onset temperature have shifted to a lower temperature. In addition to these changes in the position of the first peak, the peak height and width

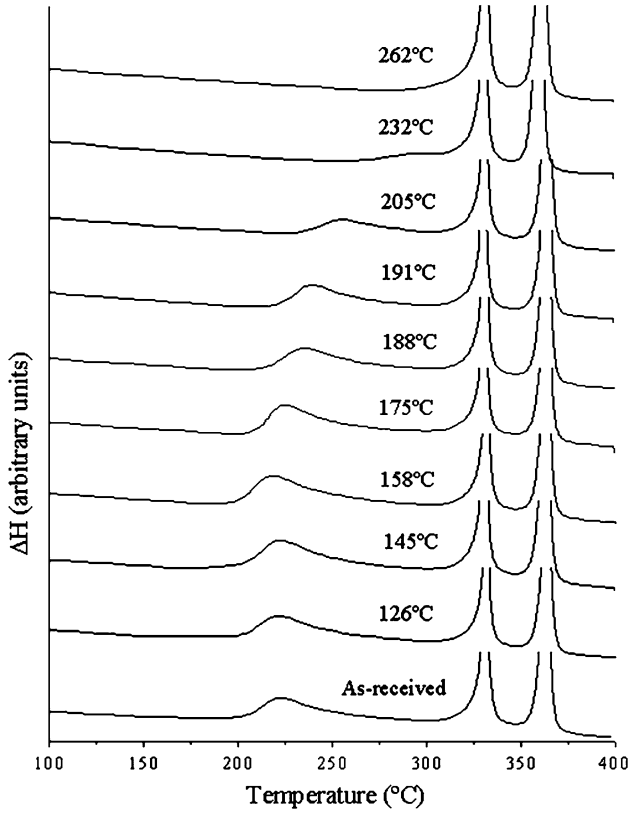

Fig. 3—DSC traces for ribbon specimens isothermally annealed for 30 min at atmospheric pressure.

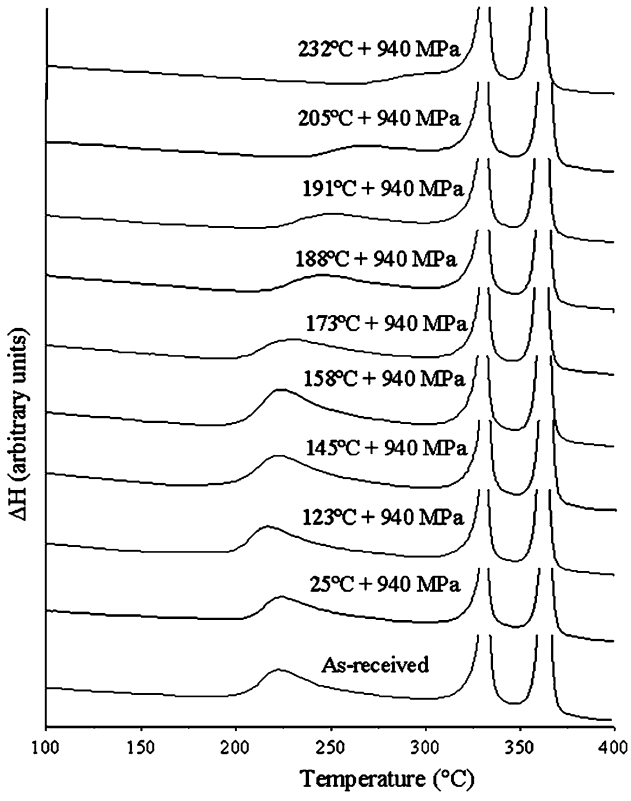

Fig. 4—DSC traces for the ribbon specimens isothermally annealed for 30 min with 940 MPa pressure.

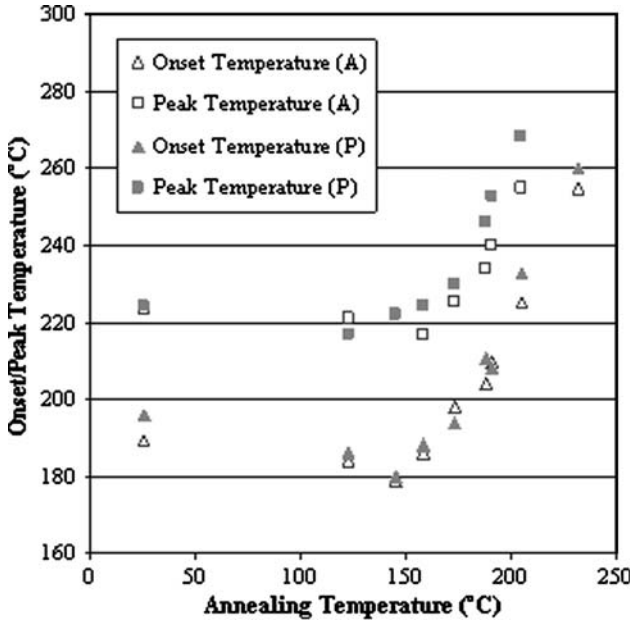

Fig. 5—Plot of onset and peak temperature *vs* annealing temperature: (A) denotes isothermal anneal at atmospheric pressure, and (P) denotes isothermal anneal with 940 MPa pressure.

were also affected. Only slight changes in the position of the second peak were observed, while the third peak was unaffected by all of the treatments given.

Particle size distributions of the α-Al nano-crystals obtained *via* TEM analysis[14] are plotted in Figure 6 for specific heat treatments. These particle size distributions were obtained from bright-field TEM images in the manner summarized elsewhere.[14] Volume fraction estimates of α-Al were obtained on specific specimens using all three techniques (*i.e.*, XRD, DSC, and TEM) following conventional procedures, as described elsewhere.[14] The results summarized in Table I show significant differences in the estimation of α-Al volume fraction, as discussed previously[14] and again subsequently.

The effects of annealing and annealing with 940 MPa pressure for 30 minutes on the microhardness are shown in Figure 7. The as-received ribbon specimens exhibited a Vickers microhardness of 3.33 ± 0.08 GPa. A slight increase in microhardness was observed after annealing at 158 °C, with much greater increases in microhardness accompanying the higher temperature annealing treatments, reaching a peak in Vickers microhardness of 5.76 ± 0.04 GPa after isothermal annealing at one atmosphere at 262 °C. Annealing for 30 minutes with 940 MPa pressure produced greater increases in microhardness than that obtained by annealing at atmospheric pressure. No cracking was observed around any of the microhardness indentations.

Complementary uniaxial tension tests exhibited engineering stress *vs* displacement traces which were linear to failure under all of the conditions tested. Multiple tests were conducted for the as-received (*i.e.*, as-melt-spun) ribbons, and only single experiments were performed on the annealed ribbon specimens. In general,

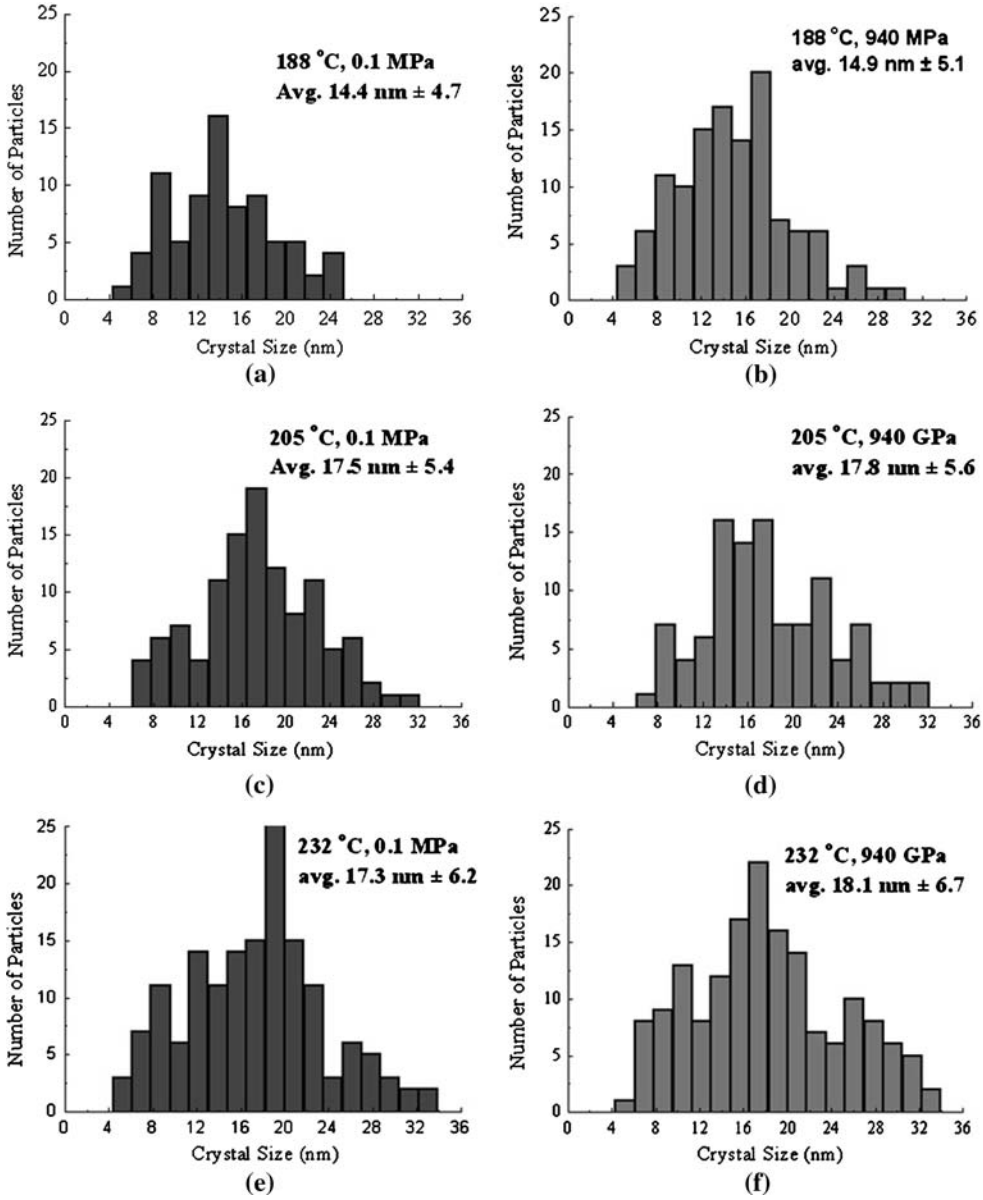

Fig. 6—Particle size distribution for ribbon specimens isothermally annealed with and without 940 MPa pressure.[3,13,14].

Table I. Volume Fractions Estimated from XRD, DSC, and TEM Analyses

Annealing Temperature	Volume Fraction XRD	Volume Fraction DSC	Volume Fraction TEM
As-received	0	0 pct	0 pct
188 °C	7.7 pct	−1.9 pct	0.41 ± 0.07 pct
205 °C	17.9 pct	13.5 pct	0.70 ± 0.14 pct
232 °C	41.0 pct	39.0 pct	1.0 ± 0.2 pct
188 °C + 940 MPa	13.8 pct	11.4 pct	0.60 ± 0.03 pct
205 °C + 940 MPa	20.6 pct	24.9 pct	0.83 ± 0.20 pct
232 °C + 940 MPa	41.5 pct	40.5 pct	1.1 ± 0.25 pct

annealing at temperatures lower than 173 °C produced fracture strengths in the range of those exhibited by the as-received ribbons, which were 968 ± 102 MPa. Ribbon specimens annealed at 123 °C, 158 °C, 173 °C, and 188 °C exhibited fracture strengths of 881, 802, 677, and 329 MPa, respectively. Ribbon specimens subjected to higher annealing temperatures exhibited premature fracture in the grip regions and during assembly of the tensile test. Fracture surfaces of the ribbons given the different annealing treatments at atmospheric pressure are shown in Figures 8(a) through (d). A transition from a single vein in the as-received sample (Figure 8(a)) to multiple veins in the sample annealed at 191 °C (Figure 8(d)) is evident. The sample annealed at 145 °C (Figure 8(b)) appears to exhibit ductile rupture and necking to a point, while a transition to multiple vein pattern is evident in the sample annealed at 173 °C (Figure 8(c)). The surfaces (*i.e.*, wheel side and air side) of the ribbons also exhibited somewhat different characteristics with regard to the extent of shear banding

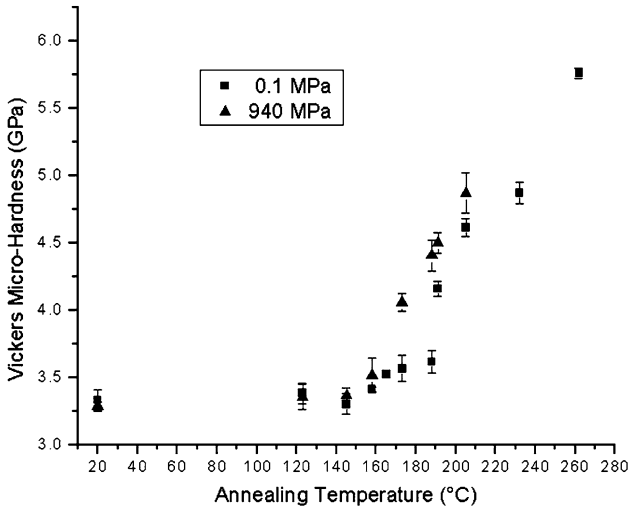

Fig. 7—Vickers microhardness (indentation load = 50 g) *vs* annealing temperature. Samples annealed for 30 min at atmospheric pressure (*i.e.*, 0.1 MPa) and 940 MPa pressure.

present near the fracture surfaces. Significantly less shear banding was evident near the fracture surface for samples annealed to contain detectable levels of α-Al particles.

IV. DISCUSSION

The various analytical techniques used in this work and related work[14,17] reveal that annealing at temperatures greater than 173 °C produces significant levels of hardening and the evolution of α-A1 particles. However, annealing at temperatures less than 158 °C failed to reveal any evidence of α-aluminum particles, yet consistent changes to both the XRD (*cf.* Figure 1) and DSC curves (*cf.* Figure 3) were exhibited at these lower annealing temperatures. The lack of detectable α-A1 precipitation in these regimes strongly suggests that the changes occurring in these regimes are due to structural relaxation, as reviewed by Greer.[18] In this regime, loss of free volume that was quenched-in during the melt-spinning process generally occurs. Attempts at measuring these changes in free volume *via* precision density measurements were not successful in the present materials due to the small amounts of material involved, as reviewed elsewhere.[19] Microhardness and tensile strength changes prior to the detectable precipitation of the α-aluminum particles are minor in the present work, consistent with expectations and published reviews.[18] However, changes to the fracture surface morphology from that exhibited by the as-quenched material to that of the relaxed specimens were detected.[19] A transition from a single vein, characteristic of fully amorphous ribbons, to that of ductile rupture (*cf.* Figures 8(a) and (b)) in the relaxed samples was consistently observed in these ribbons.

The superposition of hydrostatic pressure during annealing clearly enhances the evolution of the α-aluminum particles in the present work. This is particularly evident in the temperature regime near the onset temperature of crystallization, obtained from DSC measurements.[3,13] Although the exact mechanism whereby pressure-enhanced particle evolution has not been determined in the present work, others have shown[21,22] that pressure may enhance structural relaxation, a precursor to other types of structure evolution (*e.g.*, precipitation, phase separation, *etc.*) in amorphous systems. In addition, work by Ye and Lu[23] has indicated that applied pressure enhances the first primary crystallization peak of $Al_{89}La_6Ni_5$, with decreases to the crystallization temperature accompanying increases in superimposed pressure. This effect of pressurization on the crystallization kinetics in $Al_{89}La_6Ni_5$ was attributed[23] to the volume change during the transformation in the early stages of crystallization in that system. The present work and previous work in References 3 and 14 are consistent with this, suggesting that similar effects occur in $Al_{87}Ni_7Gd_6$.

The evolution of the α-aluminum particles accompanies large increases in microhardness without fracture around the indents in the annealed ribbons, although this strength increase was not always reflected in the uniaxial tensile results. The hardness data in Figure 7 clearly show an increase in microhardness with annealing temperatures greater than 173 °C, coincident with the evolution of appreciable levels of α-aluminum particles.[3,14] One possible source of strengthening[24] relates to the enrichment in solute content of the amorphous matrix, which arises due to the evolution of the essentially pure[17] aluminum particles. The increase in solute content of the matrix was estimated *via* knowledge of the volume fraction of α-aluminum particles, their size, and their chemistry (*i.e.*, essentially pure Al). The calculation assumes that the rejected solute is uniformly distributed in the remaining amorphous matrix, although it is known that there is solute buildup near the interfaces.[17] Figure 9 plots the microhardness of the annealed ribbons *vs* the solute content of the remaining amorphous matrix, estimated using the volume fraction of α-aluminum particles determined by XRD (Table I). It has been proposed[24] that a linear relation could exist for such behavior, and this is observed presently over a wide range of microhardness/solute contents, although the specimen annealed at 232 °C (*i.e.*, solute content 23 pct) diverges from this relation. Additional TEM is underway to determine the possible source(s) of this divergence. The deviation from a linear dependence could also suggest that matrix solute strengthening is not the sole source of annealing-induced strengthening for this material. The possibility of α-Al particle strengthening should also be explored, although this would require the evaluation of heat treatments, α-Al vol pct, α-Al particle spacings beyond that conducted presently.

Although the microhardness continued to increase with continued annealing at higher temperatures (Figure 7), the uniaxial tensile strength did not follow this trend and the ribbons were embrittled (*i.e.*, loss of strength) at the higher annealing temperatures. In part, this observation is due to the entirely different stress states experienced by the indented ribbon and that when tested in uniaxial tension. The former is deformed under

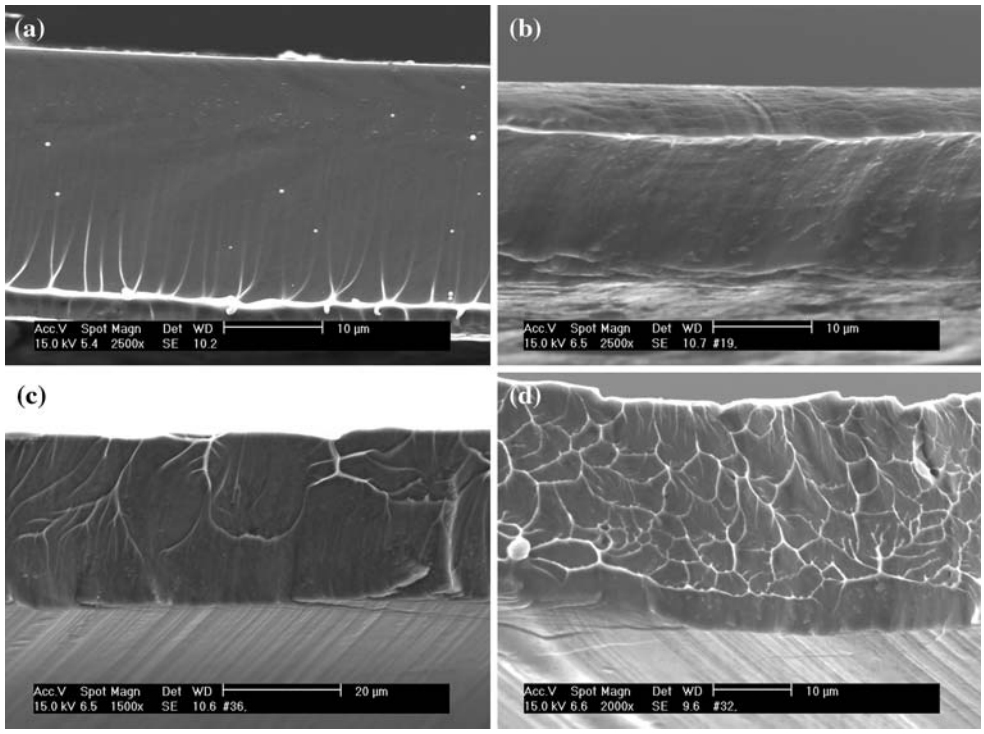

Fig. 8—Fracture surfaces of (*a*) as-received, (*b*) annealed at 145 °C at atmospheric pressure, (*c*) annealed at 173 °C at atmospheric pressure, and (*d*) annealed at 191 °C at atmospheric pressure. The entire thickness of each ribbon sample is shown.

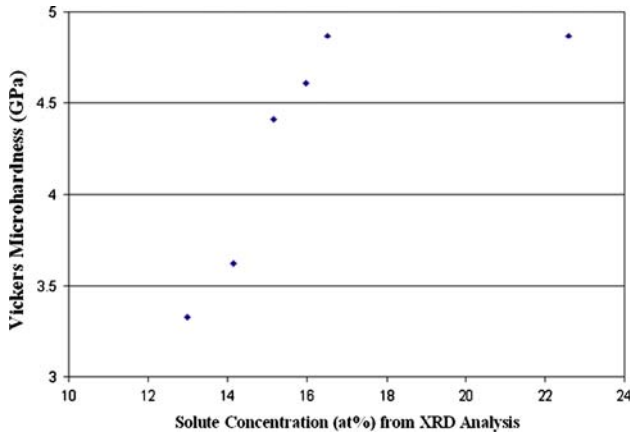

Fig. 9—Vickers microhardness of annealed ribbons *vs* solute concentration of remaining amorphous aluminum alloy matrix. Calculations of solute concentration assuming complete and uniform rejection of solute (*i.e.*, Ni and Gd) from α-Al particles into surrounding amorphous matrix. Volume fraction of α-Al obtained from XRD results (Table I).

conditions of compression plus high superimposed compression, while the latter is deformed under conditions of tension plus some level of hydrostatic tension.[16] Slight irregularities and scratches on the ribbon surfaces may significantly affect the initiation of fracture in the tension test, while not significantly affecting that of the hardness. It is also possible that the solute enrichment of the remaining matrix occurs to such an extent as to embrittle the ribbon when tested in tension but not under indentation, as discussed previously and reviewed by others.[22] Solute rejection into the matrix produces significant changes to the chemistry, which is known to affect the elastic constants of amorphous metals.[25] Recent reviews[25] have shown a correlation of embrittlement with changes in elastic constants (μ, B, and ν) in various amorphous metal systems. Solute rejection of Ni and Gd into the $Al_{87}Ni_7Gd_6$ matrix could increase the shear modulus to such an extent that brittle fracture is promoted. The higher hardness accompanying annealing is a reflection of the increased shear modulus of the matrix, although there may also be some contributions to the strength from the presence of the α-Al particles, as indicated previously.

V. CONCLUSIONS

The effects of isothermal annealing and annealing with superimposed pressure on the evolution of structure and resulting properties of amorphous $Al_{87}Ni_7Gd_6$ ribbons have been determined. The results to date indicate the following.

1. Mechanical evaluation of amorphous (*i.e.*, as-melt-spun) ribbons *via* microhardness testing and tension testing produced values of 3.3 ± 0.08 GPa and tensile strengths of 968 ± 102 MPa
2. Isothermal annealing for 30 minutes at $T < 158$ °C produced subtle changes of the first XRD peak and subtle changes to the first peak in the DSC traces, without any detectible TEM evidence of α-aluminum precipitation in the matrix. Mechanical properties such as microhardness and tensile strength were

within the range exhibited by the as-received (*i.e.*, as-melt-spun) ribbons, suggesting that the primary effects of annealing at $T < 158$ °C were structural relaxation of the glass.

3. Annealing at $T > 158$ °C produced sharpening of the first XRD peak and evolution of the second XRD peaks, along with distinct changes to the first and second DSC peaks. Significant increases in microhardness were exhibited, while limited tensile results revealed embrittlement *via* a reduction in the stress at fracture. This was attributed, in part, to the differences in stress state between compression and tension testing, as well as to the presence of scratches/imperfections on the specimen surfaces. Solute rejection into the matrix will also increase the critical elastic constants (*e.g.*, μ/B), which appear to control the intrinsic plasticity *vs* brittleness of amorphous metals, as discussed elsewhere.[25]
4. Isothermal annealing with pressure appears to accelerate the relaxation of the glass and subsequent precipitation of α-aluminum particles. Consistent changes to the XRD, DSC, and mechanical properties (*i.e.*, microhardness and tensile strength), along with the supporting TEM work,[3,14] clearly show this.

ACKNOWLEDGMENTS

Support for this work was provided by the DARPA SAM program *via* a subcontract with Boeing and Pratt & Whitney. The work has been approved for public release, and its distribution is unlimited. Discussions with A.L. Greer are gratefully acknowledged. The assistance of Professor Hala Hassan in manuscript preparation is also appreciated.

REFERENCES

1. Y. He, S.J. Poon, and G.J. Shiflet: *Science*, 1988, vol. 241, pp. 1640–42.
2. A.L. Greer: *Science*, 1995, vol. 267, pp. 1947–53.
3. B.C. Ko, P. Wesseling, O.L. Vatamanu, G.J. Shiflet, and J.J. Lewandowski: *Intermetallics*, 2002, vol. 10, pp. 1099–1103.
4. F.Q. Guo, S.J. Poon, and G.J. Shiflet: *Scripta Mater.*, 2000, vol. 43, pp. 1089–95.
5. J.C. Foley and J.H. Perepezko: *J. Non-Crystalline Solids*, 1996, vols. 205–207, pp. 559–62.
6. M.C. Gao and G.J. Shiflet: *Intermetallics*, 2002, vol. 10, pp. 1131–39.
7. B. Yao, H.C. Guo, J. Wang, B.Z. Ding, H. Li, A.M. Wang, and Z.Q. Hu: *Physica B*, 1996, vol. 228, pp. 379–82.
8. X.J. Gu, F. Ye, F. Zhou, and K. Lu: *Mater. Sci. Eng. A*, 2000, vol. 278, pp. 61–65.
9. W.H. Wang, D.W. He, D.Q. Zhao, and Y.S. Yao: *Appl. Phys. Lett.*, 1999, vol. 75, pp. 2770–72.
10. F. Ye and K. Lu: *Acta Mater.*, 1998, vol. 46, pp. 5965–71.
11. T. Imura, M. Suwa, and K. Fuji: *Mater. Sci. Eng. A*, 1988, vol. 97, pp. 247–51.
12. J.Z. Jiang, T.J. Zhou, H. Rasmussen, U. Kuhn, J. Eckert, and C. Lathe: *Appl. Phys. Lett.*, 2000, vol. 77, pp. 3553–55.
13. P. Wesseling, B.C. Ko, L.O. Vatamanu, J.B. Caris, and J.J. Lewandowski: in *Supercooled Liquids, Glasses Transition and Bulk Metallic Glasses*, *MRS Symposium Proceedings*, T. Egami, A.L. Greer, A. Inoue, and S. Ranganathan, eds., Materials Research Society, Warrendale, PA, 2003, vol. 754, pp. 365–71.
14. P. Wesseling, B.C. Ko, and J.J. Lewandowski: *Scripta Mater.*, 2003, vol. 48, pp. 1537–41.
15. H. Chen, Y. He, G.J. Shiflet, and S.J. Poon: *Scripta Metall.*, 1991, vol. 25, pp. 1421–24.
16. J.J. Lewandowski and P. Lowhaphandu: *Int. Mater. Rev.*, 1998, vol. 43, pp. 145–88.
17. R.E. Hackenberg, H.C. Jao, L. Kaufman, and G.J. Shiflet: *Acta Mater.*, 2002, vol. 50, pp. 2245–58.
18. A.L Greer: in *Rapidly Solidified Alloys*, Howard H. Liebermann, ed., Marcel Dekker, Inc., New York, NY, 1993, pp. 269–301.
19. P. Wesseling: Master's Thesis, Case Western Reserve University, Cleveland, OH, 2004.
20. F. Spaepen: *Acta Metall.*, 1977, vol. 25, pp. 407–15.
21. G. Ruitenberg, H.P. De, F. Sommer, and J. Sietsma: Phys. Rev. Lett., 1997, vol. 79, pp. 4830–33.
22. J. Sietsma, G. Ruitenberg, H.P. De, and F. Sommer: *Mat. Sci. Eng. A.*, 1997, vols. 226–228, pp. 397–400.
23. F. Ye and K. Lu: *Acta Mater.*, 1999, vol. 47, pp. 2449–54.
24. Z.C. Zhong, X.Y. Jiang, and A.L. Greer: *Mater. Sci. Eng. A*, 1997, vols. 226–228, pp. 531–35.
25. J.J. Lewandowski, W.H. Wang, and A.L Greer: *Philos. Mag. Lett.*, 2005, vol. 85, pp. 77–87.